



An Approach to Statistical Spatial-Temporal Modeling of Meteorological Fields

Mark S. Handcock & James R. Wallis

To cite this article: Mark S. Handcock & James R. Wallis (1994) An Approach to Statistical Spatial-Temporal Modeling of Meteorological Fields, Journal of the American Statistical Association, 89:426, 368-378, DOI: [10.1080/01621459.1994.10476754](https://doi.org/10.1080/01621459.1994.10476754)

To link to this article: <https://doi.org/10.1080/01621459.1994.10476754>



Published online: 27 Feb 2012.



Submit your article to this journal [↗](#)



Article views: 216



View related articles [↗](#)



Citing articles: 16 View citing articles [↗](#)

An Approach to Statistical Spatial-Temporal Modeling of Meteorological Fields

Mark S. HANDCOCK and James R. WALLIS*

In this article we develop a random field model for the mean temperature over the region in the northern United States covering eastern Montana through the Dakotas and northern Nebraska up to the Canadian border. The readings are temperatures at the stations in the U.S. historical climatological network. The stochastic structure is modeled by a stationary spatial-temporal Gaussian random field. For this region, we find little evidence of temporal dependence while the spatial structure is temporally stable. The approach strives to incorporate the uncertainty in estimating the covariance structure into the predictive distributions and the final inference. As an application of the model, we derive posterior distributions of the areal mean over time. A posterior distribution for the static areal mean is presented as a basis for calibrating temperature shifts by the historical record. For this region and season, the distribution indicates that under the scenario of a gradual increase of 5°F over 50 years, it will take 30–40 winters of data before the change will be discernible from the natural variation in temperatures.

KEY WORDS: Bayesian statistics; Climatic change; Gaussian random fields.

1. INTRODUCTION

There has been much interest recently in climatic change and potential global warming. Of central focus is the phenomenon popularly called the “greenhouse effect”: the heating of the earth via the entrapment, by certain gases, of long-wave radiation emitted from the earth’s surface. This effect produces a global mean temperature of about 59°F rather than an estimated –6°F in the absence of atmosphere (Mitchell 1989). Increasing concentrations of the gases thought to contribute to this effect have led to concern in the scientific community about temperature increases and the resulting climatic effects.

There appears to be no clear-cut consensus on the extent of global warming over the last century; most estimates run from 0.5°F to 1.0°F. The difficulty is the lack of good long-term data over large regions. The global temperature constantly changes on time scales of tens of thousands of years. In fact there have been times in the past millennium when it has been much warmer than the temperatures discussed in most global warming scenarios. The objective here is the statistical validation of a postulated rapid change over the next century that will have enormous environmental impact.

Much of the evidence for a global warming effect has been based on large-scale general circulation models (GCM’s), which use multilevel mathematical representations of the atmosphere for weather prediction. Given the complexity of the environment and the relative simplicity of the models, there is much controversy concerning their validity. Results from the four most widely cited GCM’s from the National Center for Atmospheric Research (NCAR), Geophysical Fluid Dynamics Laboratory (GFDL) of the National Oceanographic and Atmospheric Administration, the Goddard Institute of Space Studies (GISS), and the Hadley Center for Climate Prediction and Research at Bracknell, England, are

still far from being in agreement, although all models predict higher winter temperatures at the higher northern altitudes as a function of increasing greenhouse gases.

Significant global warming would have an enormous effect on the environment and the world economy. Altering the world economy to reduce the production of the gases suspected of increasing the greenhouse effect would be very costly and/or drastically alter our way of life. Some argue that the political decision is best postponed until after the empirical evidence is in. This article sheds light on how long we would have to wait to detect a global warming with sufficiently high confidence to support such a decision.

In this paper we develop spatial-temporal models for temperature fields over a region in the northern United States covering eastern Montana through the Dakotas (90°–107° in longitude) and northern Nebraska up to the Canadian border (41°–49° in latitude). We choose the winter months and this region as our study area because GCM predictions of climatic change (4°F–10°F) induced by increased greenhouse gases are expected to be at maximum for high latitudes during the winter months (IPCC 1990; Mitchell 1989). In addition, the relatively stable and simple topography of the region help ensure homogeneity and the minimization of localized effects. Data from the United States historical climatological network, reported by Quinlan, Karl, and Williams (1987) is used to explore long-term changes and potential effects of increased greenhouse gas concentrations.

There is much interest in empirical studies of climatic change. Jones et al. (1986) considered station data to investigate long-term variation in the surface temperature of the northern hemisphere. Karl (1984, 1985) considered climate variation and change in North America. These studies emphasized the dynamic nature of the climate system and the existence of abnormal winter temperatures within the climate system. Other empirical work was reported by Diaz and Quayle (1978, 1980). A hindrance to these and earlier studies has been the dearth of quality data with both spatial and temporal extent.

* Mark S. Handcock is Assistant Professor of Statistics, Department of Statistics & Operations Research, Leonard N. Stern School of Business, New York University, NY 10012. James R. Wallis is Research Scientist, Department of Mathematical Sciences, IBM T. J. Watson Research Center, Yorktown Heights, NY 10598. This article was originally presented at the Copenhagen General Assembly of the European Geophysical Society, April 1990. The authors thank Paul Switzer, Noel Cressie, Roderick Little, the associate editor, and three referees for numerous useful comments that have greatly improved this article.

Karl, Heim, and Quayle (1991) considered a similar region with the objective of identifying greenhouse effects. They constructed a pure time-series model for the averages of the stations enclosed in the region and did not address the spatial aspects of the temperature field. In contrast, this article develops a comprehensive model for the spatial dimension in conjunction with the temporal component. In addition, the model is for the meteorological field as a whole, rather than just a particular characteristic. This is important, as it facilitates direct comparison with GCM's and prediction of derived quantities throughout the region and over time. In particular, it allows the prediction of the meteorological field at each location (e.g., city or county) with an associated assessment of the quality of prediction.

The traditional best linear unbiased prediction (BLUP) procedure, also known as "kriging," is used in this article for inference, but within a Bayesian framework. Particular attention is paid to the treatment of parameters in the covariance structure and their effect on the quality, both real and perceived, of the prediction.

Our approach is to use posterior distributions for the static areal quantities as a basis for calibrating temperature shifts by the historical record. In particular, the objective is to understand how soon gradual increases in temperature over this region would be discernible from the year-to-year variation.

1.1 U.S. Historical Climatology Network

Recently the U.S. Carbon Dioxide Information Analysis Center established a network of 1,219 stations (the HCN network) for the contiguous United States "with the objective of compiling a data set suitable for the detection of climatic change" (Quinlan, Karl, and Williams 1987, p. 1). The network record includes maximum, minimum, and mean monthly temperatures and total monthly precipitation since the 1890s. The data base is available through the National Climate Data Center (NCDC).

Much attention has been given to the quality issues in terms of the choice of stations in the network (e.g., locations away from urban areas and the identification of artificial changes in local environment). The data from selected station records have been meticulously cleaned using procedures to check consistency with neighboring stations and temporal homogeneity.

As part of a study to improve the land surface parameterization of the GFDL GCM, a 41-year daily-value data base was prepared and made available in CDROM format (Wallis, Lettenmaier, and Wood 1991). The study used 1,036 of the original HCN stations, with missing days flagged and then estimated by correlation to nearby stations. There are differences between the unadjusted monthly mean values reported by Karl, Williams, Quinlan, and Boden (1990) and those reported by Wallis et al. (1991). Some of these differences can be accounted for by a difference in the treatment of missing days. Karl et al. (1990) summed the observed days in any given month and divided by their number to calculate the average monthly value; missing days were not estimated. Wallis et al., however, encountered many cases where even the number of missing days in a given month

did not agree between the daily and monthly NCDC data bases. The data used in this study are that given by Wallis et al., and the sites used were chosen so as to minimize the effect of these data peculiarities. There are minor changes to many of the numerical results, but the inference has been largely unchanged. The reformulated data appear to remove an additional source of "random" variation from the HCN data set. If the NCDC ever prepares a cleaned-up data base, then the calculations reported here could easily be repeated. In the interim, we do not believe that data errors for the stations and periods used in this study are large enough to invalidate any of our results or conclusions.

2. ANALYSIS OF SPATIAL STRUCTURE

In this section we discuss a spatial model appropriate for a meteorological field over a single time period. The field discussed here is the average winter temperature. The daily average temperature at a location is defined to be the mean of the daily maximum and the daily minimum at that location. The average winter temperature is defined to be the average daily average temperature over the months December, January, and February using the data and aggregation method of Wallis et al. (1991). For example, winter for the year 1983 starts in December 1983.

The generalizations to include a temporal component is the subject of the following section.

Figure 1 represents the region under study. The locations of the 88 U.S. historical climatological network stations in the region are marked with "+." The elevation of the stations, in feet, are represented by the overlaying gray-scale image.

Note that the elevation increases from east to west and also from north to south. As expected, the elevation of the station has a marked impact on temperature, and it is essential that the model reflect this relationship.

Figure 2 is a gray-level image of the mean winter temperatures for winter 1983–1984. These data are the basis for the spatial analysis described in this section.

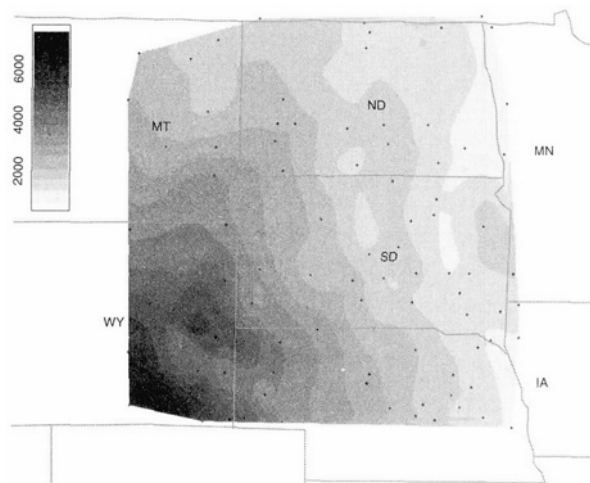


Figure 1. Locations and Elevations of the U.S. Historical Climatological Network Stations. The gray-level image is for the elevation above sea level over the region.

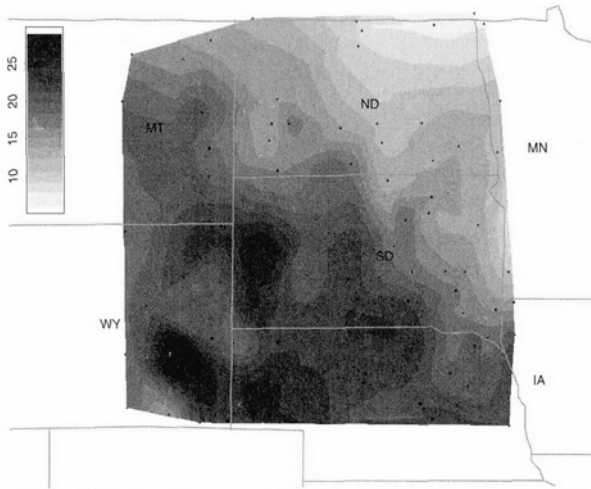


Figure 2. Gray-Level Image of the Mean Winter Temperatures for the Winter of 1983-1984. The temperature range, in Fahrenheit, is given in the legend.

Suppose that $Z(\mathbf{x})$ is a real-valued stationary Gaussian random field on the region under study (\mathbf{R}) with mean

$$E\{Z(\mathbf{x})\} = \mathbf{f}(\mathbf{x})'\boldsymbol{\beta},$$

where $\mathbf{f}(\mathbf{x}) = \{f_1(\mathbf{x}), \dots, f_q(\mathbf{x})\}'$ is a known vector function and $\boldsymbol{\beta}$ is a vector of unknown regression coefficients. Furthermore, the covariate function is represented by

$$\text{cov}\{Z(\mathbf{x}), Z(\mathbf{y})\} = \alpha K_\theta(\mathbf{x}, \mathbf{y}) \quad \text{for } \mathbf{x}, \mathbf{y} \in \mathbf{R},$$

where $\alpha > 0$ is a scale parameter, $\boldsymbol{\theta} \in \Theta$ is a $q \times 1$ vector of structural parameters, and Θ is an open set in \mathbb{R}^p . The division is purely formal, as $\boldsymbol{\theta}$ may also determine aspects of scale. This formulation is standard for meteorological networks (Gandin 1963).

We observe, from a single realization of the field, $\{Z(\mathbf{x}_1), \dots, Z(\mathbf{x}_n)\}' = \mathbf{Z}$, where $\mathbf{x}_1, \dots, \mathbf{x}_n$ are the spatial locations of the stations in the network. In our situation, each of the $n = 88$ observations is the average winter temperature at a site for a winter. We will focus on the prediction of $Z(\mathbf{x}_0)$, where \mathbf{x}_0 is a new location in the region of interest.

The kriging predictor is the BLUP of the form $\hat{Z}_\theta(\mathbf{x}_0) = \boldsymbol{\lambda}(\boldsymbol{\theta})'\mathbf{Z}$; that is, the unbiased linear combination of the observations that minimizes the variance of the prediction error. The quality of the prediction is determined by the distribution of the prediction error, $e(\mathbf{x}_0) = Z(\mathbf{x}_0) - \hat{Z}_\theta(\mathbf{x}_0)$. Note that the underlying kriging procedure is motivated by sampling considerations, producing point predictions and associated measures of uncertainty for those predictions, both based on sampling distributions unconditional on the observed \mathbf{Z} . It is well known, however, that kriging can be given a Bayesian interpretation when the mean is of known regression form (see for example, Omre and Halvarsen 1989, Handcock and Stein 1993; and Hastie and Tibshirani 1990).

Implementation of this model requires the specification of the regression function $\mathbf{f}(\mathbf{x})$ and the spatial covariance structure $K_\theta(\cdot, \cdot)$. The components of $\mathbf{f}(\mathbf{x})$ should be easily measurable spatial characteristics of the station, such as the

latitude, longitude, and elevation of each station. Other possibilities are polynomials in latitude, longitude, elevation, and the distance to the closest urban area or transformations of them. The ultimate choices for components for the mean function were latitude, longitude, and elevation, as additional components did not have an appreciable effect on the likelihood ratios or on the likelihood function itself (see Secs. 2.2 and 2.3). Specification of the covariance structure is covered in the following section.

2.1 Spatial Correlation Structure: The Matérn Class

The properties of the covariance function directly determine the properties of the random field model. If the class describes too narrow a range of behaviors of the random field or is not parsimonious, it will not provide an adequate basis for modeling. This goes beyond the criterion of pleasing visual shape typically used to choose covariance classes. In this section we describe a general class of isotropic and homogeneous covariance functions that we feel provides a sound foundation for the parametric modeling of Gaussian random fields. An isotropic and homogeneous covariance function can be represented as a function of $|\mathbf{x} - \mathbf{y}|$, the distance between \mathbf{x} and \mathbf{y} , for all $\mathbf{x}, \mathbf{y} \in \mathbf{R}$. The class is motivated by the smooth nature of the spectral density, the wide range of behaviors covered, and the interpretability of the parameters (Handcock and Stein 1993; Matérn 1986). The Matérn class is characterized by the parameter $\boldsymbol{\theta} = (\theta_1, \theta_2)$. $\theta_1 > 0$ is a scale parameter controlling the spatial range of correlation, while the smoothness parameter $\theta_2 > 0$ directly controls the smoothness of the random field. The exponential class corresponds to the subclass with smoothness parameter $\theta_2 = \frac{1}{2}$; that is,

$$\exp(-|\mathbf{x} - \mathbf{y}| \sqrt{2}/\theta_1).$$

The subclass defined by $\theta_2 = 1$ was introduced by Whittle (1954) as a model for two-dimensional fields and it is commonly used in hydrology (Creutin and Obled 1982; Jones 1989; Mejía and Rodríguez-Iturbe 1974). As $\theta_2 \rightarrow \infty$, $K_\theta(\mathbf{x}, \mathbf{y}) \rightarrow \exp(-|\mathbf{x} - \mathbf{y}|^2/\theta_1^2)$, often called the "Gaussian" covariance function. We shall refer to it as the squared exponential model. This model forms the upper limit of smoothness in the class and will rarely represent natural phenomena, as realizations from it are infinitely differentiable.

The spectral density at frequency $\boldsymbol{\omega}$ on \mathbb{R}^d has the general form

$$\frac{\alpha \cdot c(\boldsymbol{\theta}, d)}{[1 + (\theta'_1 \boldsymbol{\omega})^2]^{\theta_2 + d/2}},$$

where the constant

$$c(\boldsymbol{\theta}, d) = \frac{\theta_1^d \Gamma(\theta_2 + d/2) (4\theta_2)^{\theta_2}}{\Gamma(\theta_2) \pi^{d/2}} \quad \text{and} \quad \theta'_1 = \theta_1 / (2\sqrt{\theta_2}).$$

The corresponding isotropic covariance functions have the form

$$K_\theta(\mathbf{x}, \mathbf{y}) = \frac{\alpha}{2^{\theta_2 - 1} \Gamma(\theta_2)} \cdot \left(\frac{|\mathbf{x} - \mathbf{y}|}{\theta'_1} \right)^{\theta_2} \mathcal{H}_{\theta_2} \left(\frac{|\mathbf{x} - \mathbf{y}|}{\theta'_1} \right)$$

where Γ is the gamma function and \mathcal{H}_{θ_2} is the modified Bessel

function of the third kind and order θ_2 discussed by Abramowitz and Stegun (1964, sec. 9). A field with this covariance function is $\lceil \theta_2 - 1$ times (mean squared) differentiable where \lceil is the integer ceiling function. The realizations will have continuous $\lceil \theta_2 - 1$ derivatives if $\theta_2 > \lceil \theta_2 - \frac{1}{2}$. If the field is Gaussian, then the realizations will have continuous $\lceil \theta_2 - 1$ derivatives (almost certainly) (see Cramèr and Leadbetter 1967, secs. 4.2, 7.3, and 9.2–9.5). Note that these covariance functions are always positive, so that the class is inappropriate for fields with negative correlations. A general treatment has been given in the seminal work by Matérn (1986).

The calculation of \mathcal{H}_{θ_2} for nonintegral θ_2 is nontrivial. There are a number of publicly available programs to this end, including RKBESL from the SPECFUN (Cody 1987) library, available free from NETLIB (Dongarra and Du Croz 1985). Although the calculation is expensive relative to the other forms of covariance functions, this cost is negligible compared to the other computing costs involved in the analysis.

2.2 Model Development and Validation

In traditional kriging, one estimates α and θ by either likelihood methods or various ad hoc approaches. The likelihood approach to estimating the covariance structure was first applied in the hydrological and geological fields following Kitanidis (1983), Kitanidis and Lane (1985), and Hoeksema and Kitanidis (1985); see also the works of Mardia and Marshall (1984), Zimmerman and Zimmerman (1991), Handcock and Stein (1993), and Handcock (1989). Usually the predictor and the behavior of the prediction error are themselves estimated by “plugging in” the estimates to the expressions for known α and θ .

The log-likelihood of α , θ , and β , having observed \mathbf{Z} , is

$$L(\alpha, \theta, \beta; \mathbf{Z}) = -\frac{n}{2} \ln(\alpha) - \frac{1}{2} \ln(|\mathbf{K}_\theta|) - \frac{1}{2\alpha} (\mathbf{Z} - \mathbf{F}\beta)' \mathbf{K}_\theta^{-1} (\mathbf{Z} - \mathbf{F}\beta),$$

where $\mathbf{K}_\theta = \{K_\theta(\mathbf{x}_i, \mathbf{x}_j)\}_{n \times n}$, $\mathbf{F} = \{f_j(\mathbf{x}_i)\}_{n \times q}$ and the dependencies on n have been suppressed. The values of α , θ , and β that maximizes this log-likelihood are denoted by $\hat{\alpha}$, $\hat{\theta}$, and $\hat{\beta}$.

2.3 Checking the Validity of the Assumptions

The approach used here is to check the assumptions in the context of particular models. Conditional on the correctness of a particular model, there are verifiable properties that can be checked. An advantage of the likelihood-based approach to inference is that it facilitates the determination of the model’s validity. As a preliminary check, the data were screened for obvious deviations from the assumptions. Initial exploration of univariate data transformations, such as square-root and log, indicate similar results to those presented in this article based on the untransformed data.

The major assumptions implicit in the model are spatial stationarity of the Gaussian random field, isotropy of the correlations, and correct specification of the mean. These

are interdependent, so checking them individually is usually not the best approach.

The assumption of stationarity and isotropy can be checked, at least approximately, by considering the behavior of empirical variograms for small distances. The variogram of $Z(\mathbf{x})$ is

$$2\gamma(\mathbf{h}) \equiv \mathbb{V} \{Z(\mathbf{x} + \mathbf{h}) - Z(\mathbf{x})\} \quad \text{for } \mathbf{x} + \mathbf{h}, \mathbf{x} \in \mathbf{R},$$

so that $\gamma(\mathbf{h})$ describes aspects of the covariance structure. (For a discussion of variograms and their estimation, see Cressie 1991). Here variograms are estimated from the residual observations, $\mathbf{Z} - \mathbf{F}\hat{\beta}$, with respect to a candidate model. The validity of the isotropy assumption can be illuminated via empirical directional variograms (i.e., \mathbf{h} is restricted to a single direction). Consider Figure 3 as examples of such empirical directional variograms for winter 1983–1984. The east–west variogram is based on only those pairs of stations that have approximately an east–west orientation to each other. In this example this relationship is defined as only those pairs of stations whose connecting line segment makes at most a 45° angle with the east–west direction. Hence the behavior of the east–west variogram for small distances ($< 2^\circ$) represents the dependence in the east–west direction. The corresponding north–south variogram has a similar interpretation. The isotropic variogram, independent of spatial orientation, is also plotted. Substantial deviation between the two directional variograms would have provided evidence for anisotropy. Similar directional variograms were compared for noncardinal directions, providing little evidence of anisotropy.

Another approach is to consider geometric anisotropies (Matheron 1965), where $K(\mathbf{x}, \mathbf{y})$ is a function of $|\mathbf{V}\mathbf{x} - \mathbf{V}\mathbf{y}|$ for a possibly unknown 2×2 matrix \mathbf{V} . This represents a rescaling of the usual Euclidean metric. Based on changes in the likelihood, the addition of geometric anisotropies does not lead to significant improvements to the model. Based

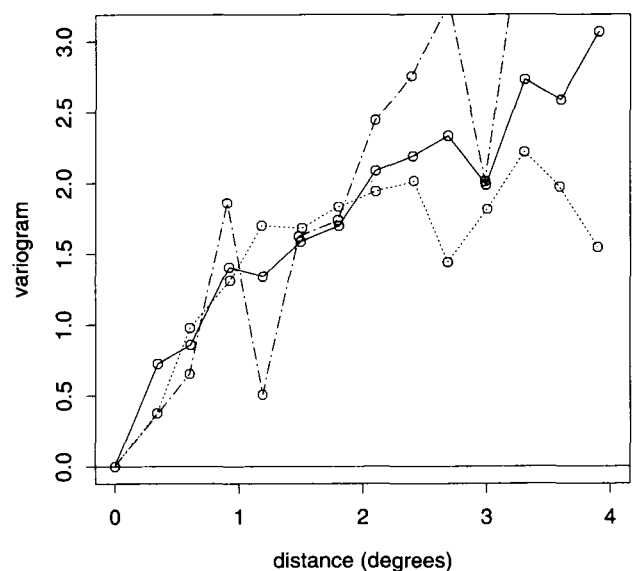


Figure 3. Empirical Variograms for the 1983–1984 Mean Winter Temperatures. —, isotropic; ·····, north-south; - - - -, east-west.

on these investigations, the homogeneous and isotropic Matérn class appeared to be appropriate.

In general, it is difficult to determine whether the temperature field is Gaussian, because the observations are spatially dependent and the correlation structure is unknown. In particular, the marginal distribution of the temperature readings is little guide to their joint distribution. Because each average winter temperature is the average of 182 minimum and maximum daily measurements, the law of large numbers should work in favor of the Gaussian assumption at the marginal level, and hopefully at the joint level as well. One check on the joint Gaussian assumption is possible using the fact that, conditional on the estimated model, the whitened residuals $\mathbf{K}_\delta^{-1/2}\{\mathbf{Z} - \mathbf{F}\hat{\beta}\}$ are independent and standard Gaussian. Hence plots of the whitened residuals against the latitude, longitude, elevation, and \mathbf{Z} itself can be interpreted in the same way as residual plots from linear regression. This assumes that the mean and covariance are correctly specified. In particular, evidence of misspecification of the mean, heterogeneity of covariance, outliers, and deviations from the Gaussian distribution can be observed. This process was carried out on all significant intermediate models, as well as on the final model. Nonstationarity of the covariance and nonstationarity of the mean are difficult to check together, and wholly satisfactory procedures have yet to be developed. One approach is to partition up the region into relatively homogeneous sub-regions and build models for each region separately.

It should be noted that this vector is not unique, and we could just as well consider any orthogonal transformation of $\mathbf{K}_\delta^{-1/2}\{\mathbf{Z} - \mathbf{F}\hat{\beta}\}$. The weakness of this check is that the whitened residuals no longer reflect the spatial information.

The underlying temperature field for a given winter is a realization of the random field and hence can be thought of as a (deterministic) surface in two dimensions. Our observations are then the values of this surface at 88 locations in the two-dimensional region. Based on meteorological arguments, we believe that the underlying temperature field is continuous and may even be differentiable as a real-valued function in two dimensions. Furthermore, for this network of stations, the magnitude of the random measurement error appears to be small relative to the winter-to-winter variation. Typically, the estimated random measurement error is 0%–5% of the point variance. There is little likelihood evidence for random measurement error, and this error is not included in this analysis, to reduce the computational and notational burden.

2.4 Modeling Within the Matérn Class

The maximum likelihood estimate for the covariance structure based on the Matérn class is $(\hat{\alpha}, \hat{\theta}_1, \hat{\theta}_2) = ((1.85^\circ\text{F})^2, 1.72^\circ, .55)$. The range of dependence (1.72°) spans approximately one-fifth of the region under study. The point standard deviation of the mean winter temperature is $\sqrt{\hat{\alpha}} = 1.3^\circ\text{F}$. The estimate of the smoothness indicates that the field is about as smooth as the “exponential” model ($\theta_2 = \frac{1}{2}$), in the sense that similar values of θ_2 correspond to similar smoothness conditions on the realizations of the random field (see Sec. 2.1).

The estimates of the regression parameters indicate that the mean winter temperature decreases by 2.9°F per degree increase in latitude. There is a 2.4°F decrease per 1,000-foot increase in elevation. In addition, for every degree increase in longitude eastward, the mean winter temperature decreases by 1.3°F . This latter effect is possibly a surrogate for the winter climatic patterns over the region.

The difficulty of using this or any other point estimate of the covariance structure as a surrogate for the “true” covariance structure is that the uncertainty in the estimate is not directly translated to the final inference. The maximum likelihood estimate may be the best single representative available, but this reduction itself can be detrimental to the inference. This approach was developed by Handcock and Stein (1993). The kriging procedure is often described as optimal (Matheron 1965), because it produces optimal predictions when the covariance structure is known. If an estimate of the covariance structure is used, then the primary motivation for kriging is in question.

One approach to include the uncertainty in the estimate is to use the Bayesian framework and base inference on the posterior distributions of the quantities of interest. This approach takes into account the complete likelihood surface rather than plugging in the maximum likelihood estimate of the covariance structure. It allows the performance of the usual plug-in predictive distribution based on an estimated covariance structure to be critiqued within a larger framework. Another non-bayesian approach is developed in Zimmerman and Cressie (1992).

The marginal posterior distribution for the smoothness parameter (θ_2) for winter 1983–1984 is given in Figure 4. An expression for the posterior distribution is given by Handcock and Stein (1993) and is based on the log-likelihood in Section 2.4.

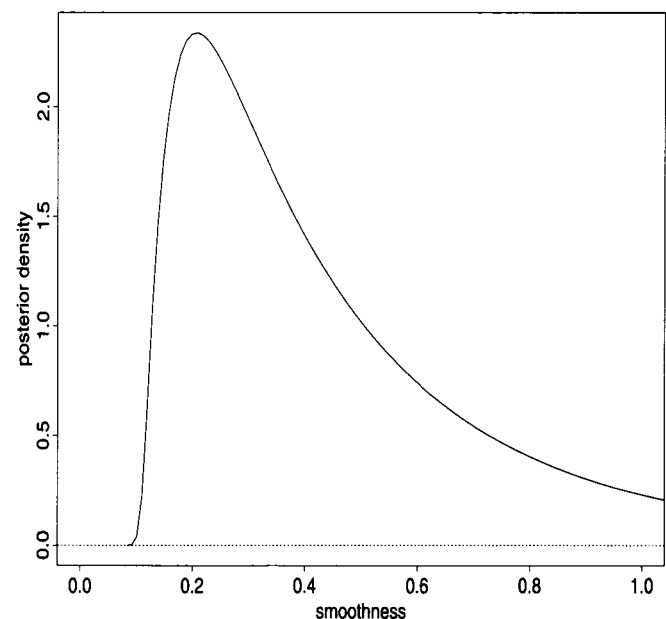


Figure 4. Posterior Distribution for the Smoothness Parameter Based on the Matérn Model.

This distribution summarizes the uncertainty we have about the smoothing parameter. The distribution has negligible mass outside of $(.1, 1.5)$, representing fields that are mean-square continuous or at most once mean-square differentiable. The marginal posterior distribution for the range (θ_1) is very flat, indicating that the range is hard to identify from the information.

The prior used here is

$$\Pr(\alpha, \beta, \theta_1, \theta_2) \propto \Pr(\theta_1)\Pr(\theta_2)/\alpha,$$

where

$$\Pr(\theta_i) = \frac{1}{(1 + \theta_i)^2}.$$

The latter prior is noninformative for $\theta_i/(1 + \theta_i)$ for $[0, 1]$. The prior reflects the belief that higher values of the smoothness, θ_2 , are a priori less likely than smaller values. The belief is that a random field is more likely to be 1 or 2 times differentiable, rather than, say, 101 times differentiable. In particular, $\theta_2 = \infty$ is given zero prior weight. A similar rationale is given for the prior on the spatial range parameter θ_1 . Clearly, the priors are chosen partly for convenience; they are reasonably flat in the region that the likelihood has mass and more closely relate to our beliefs than Jeffrey's noninformative prior

$$\Pr(\theta_i) = 1 \quad \theta_i > 0.$$

It should be emphasized that the method is designed to incorporate an informative prior if the meteorologist, hydrologist, and/or statistician has one.

As an example, suppose that we wish to summarize our knowledge of the mean temperature for winter 1983–1984 at the center of South Dakota. The predictive distribution is centered about 18.59°F and has a standard deviation of .92°F. Calculation of the predictive distribution requires two-dimensional integration where the integrand is composed of the posterior density of θ and the predictive density of the mean winter temperature at the center of South Dakota given θ . The distribution is a mixture of noncentral t distributions and for this winter is virtually indistinguishable in shape from a Gaussian distribution. (For details, see Handcock and Stein 1993).

2.5 Alternative Estimation of the Mean

This spatial analysis was repeated independently for the 50 winters from 1937–1938 to 1986–1987. Figure 5 presents a sample of the residual temperature fields, $Z(\mathbf{x}) - \mathbf{f}(\mathbf{x})'\hat{\beta}$, after subtracting off the maximum a posteriori (MAP) estimate of the mean function. The gray scales are the same for each image. The images exhibit little evidence of residual spatial trends, and the spatial arrangement of peaks and valleys differs from winter to winter.

One alternative approach to our parametric mean, $\mathbf{F}\hat{\beta}$, is to estimate the mean at each station by $\bar{Z}(\mathbf{x}_i) = \frac{1}{50} \sum_{t=1}^{50} Z_t(\mathbf{x}_i)$, the temporal average at that station. The deviation of the observations for a given winter from the temporal average would then have a mean of approximately zero. Thus we can predict the value at a site using a mean zero random

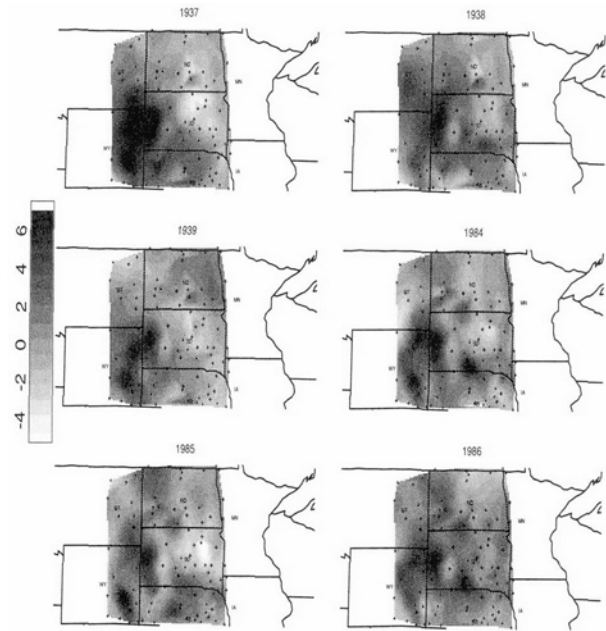


Figure 5. A Sample of the Residual Mean Winter Temperature Fields for 1937–1939 and 1984–1986.

field model for the residual covariance and add to it an estimate of the mean at that site. This is essentially the approach taken by Haslett and Raftery (1989) and is appropriate when one wants to predict at locations where one already has data, under the assumption that the mean is temporally constant and the temporal dependence is weak. In our situation we wish to predict at many locations for which data do not exist. Thus an estimate of the mean at unobserved locations appears to be necessary to be able to predict at the locations.

Our estimate of the parametric mean tends to explain a large proportion of the variation in the data. The total variation of the residual field for a winter about the parametric estimate of the mean for that winter is typically $(2^\circ\text{F})^2$. The total variation of the original field (i.e., the deviation from a constant mean) is typically $(9^\circ\text{F})^2$. The total variation of the residual field for a winter about the temporal average at that site is typically $(7^\circ\text{F})^2$. The difference is largely due to the fact that the parametric mean is estimated separately for each winter, whereas the temporal average implicitly assumes that the mean at each site is constant over time. As the latter does not appear to be the case, the temporal average does not explain much of the variation in the data.

3. ANALYSIS OF TEMPORAL STRUCTURE

In this section we consider the temporal component of the model, generalizing the random field to $Z_t(\mathbf{x})$, where $t = 1937, \dots$ represents the winter of observation. We consider the time series of data from each station, independent of the spatial information.

Figure 6 presents the time series and empirical autocorrelation functions for four spatially separate stations. Individually, the time series are quite variable over time. The

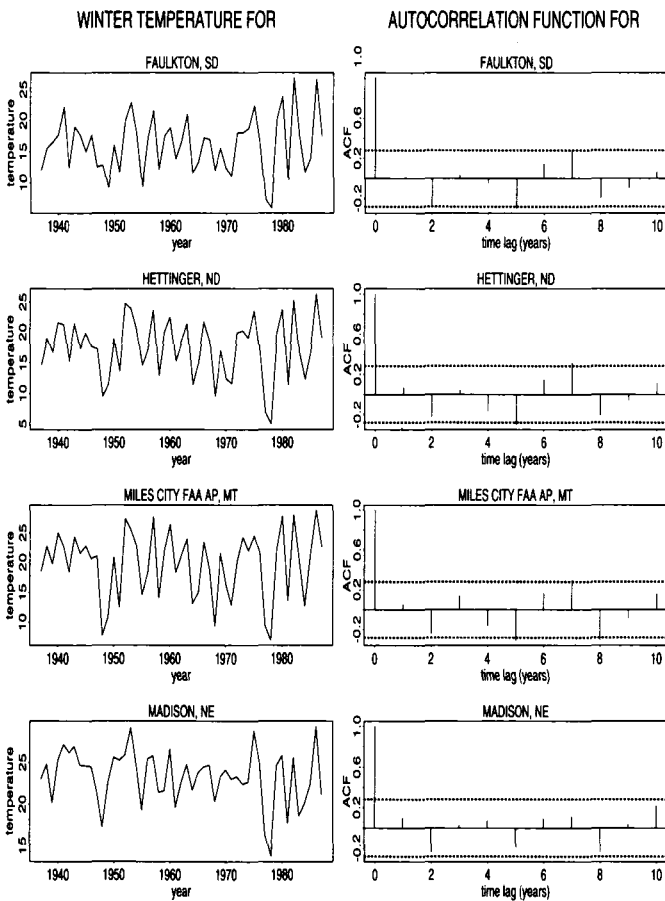


Figure 6. Time Series and Empirical Autocorrelation Functions for Four Typical Sites.

right side figures are the sample autocorrelation functions corresponding to the time series. The dashed boundaries represent approximate 95% confidence limits. Note the similar patterns in the series over time and the lack of first lag autocorrelation. The median cross-correlation is .78 with quantiles .64 and .87, indicating a tendency to move in conjunction with each other over time and reflecting the influence of the spatial correlation modeled in the previous section.

In the next two subsections we investigate these fields for short-memory and long-memory temporal structures. We find that they are close to being uncorrelated over time. We also test to see whether the spatial structure changes over time.

3.1 Short-Memory Temporal Dependency

The natural starting point in a search for short-memory dependence in a time series is fitting a first-order autoregressive (AR) model. This simple model is the natural alternative to the model of independence. The AR(1) model was fitted to the time series of each station, and the estimate of the first-lag autocorrelation was tested for statistical significance. Only 3 of the 88 stations tested were significant, indicating little evidence of AR(1) structure. The improvement to the log-likelihood from the addition of the additional parameter is minor.

How closely correlated are the effects of the spatial factors on the mean over time? To look at this, we consider the time series of estimated coefficients for each factor in Table 1. The Durbin-Watson statistic is a useful test for serial correlation in the error term of a linear model.

The Durbin-Watson statistics are derived from the multivariate time series of regression coefficients $\hat{\beta}_t$. There is moderate dependence between the time series. If the observed value of d is greater than 1.59, then we conclude that the value is insignificant at the 5% level for the test of positive serial correlation. All of the time series fail this test. If the observed value of d is greater than 2.41, then we conclude that the value is insignificant at the 5% level for the test of negative serial correlation. All of the time series fail this test as well. A multiple-comparisons adjustment could be made that would adjust for the four simultaneous tests and the dependence. The dependence makes the individual tests slightly conservative. There is little evidence of serial correlation in these time series.

3.2 Long-Memory Temporal Dependency

In the previous subsection, little evidence was found for short-term temporal dependency. In this section we consider the presence in the time series of significant dependence between observations a long time span apart. A natural way to investigate the time series for long-memory temporal dependency is to consider autoregressive integrated moving average (ARIMA) processes with nonintegral degrees of differencing, d , (ARIMA(p, d, q)). These models have been considered in the elegant and insightful papers of Hosking (1981, 1984). The idea is that the short-memory component of the series will be accounted for by the autoregressive moving average (ARMA) part of the model, and the long-memory component will be accounted for by the fractional differencing. As there appears to be little evidence for a short-memory component we will focus on the ARIMA(0, d , 0) models. The ARIMA(0, d , 0) model, consisting of $\Delta^d Z_t(\cdot)$ being independent and identically distributed zero-mean Gaussian random variables, is the fundamental model in this class (Hosking 1984).

Inference for the differencing parameter, d , can be achieved using likelihood-based inference as in the previous sections. Figure 7 presents the log-likelihood for d profiled over the scale parameter, α , and a constant mean. The station in this example is Faulkton, South Dakota. The maximum likelihood estimate is $\hat{d} = .048$, with a standard error of .09. Note that the change in log-likelihood from the maximum likelihood estimate to the model of independence ($d = 0$) is small. This provides evidence that little long-memory de-

Table 1. Durbin-Watson Statistics for the Time Series of Coefficients in the Mean Function

Component of the mean, $f(\cdot)$	Durbin-Watson statistic, d
Constant	1.75
Latitude	2.13
Longitude	2.10
Elevation	1.64

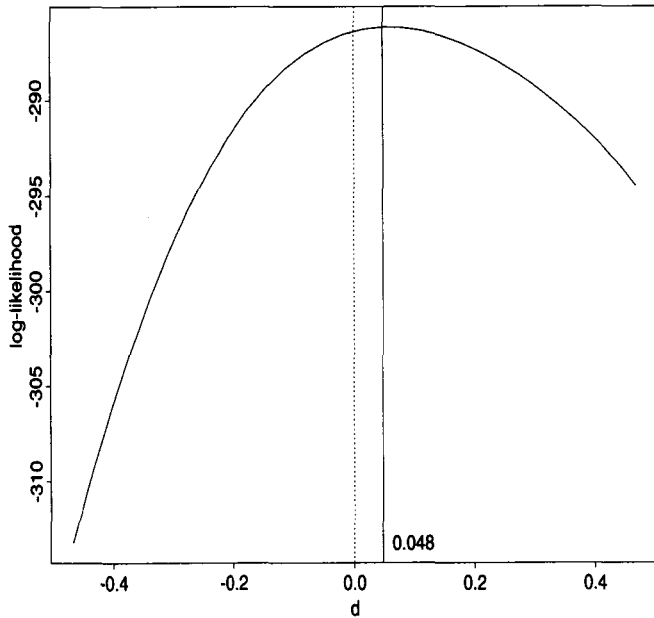


Figure 7. Profile Log-Likelihood for the Fractional Differencing Parameter, d , in the ARIMA(0, d , 0) Model for Faulkton, South Dakota.

pendency exists in the series. The above process was repeated on the directly differenced series, with the same conclusion. Similar results were also found to hold for the other stations.

In conclusion, there is little evidence of either short-memory or long-memory dependency in the time series of the stations. There also is little evidence that the spatial structure changes over the time scale considered here.

4. MEASURING AREAL MEAN TEMPERATURE

In the previous sections we found a complex spatial structure to the mean winter temperatures, little temporal dependence structure, and little evidence for changing spatial structure over time. In this section we focus interest on a measure of the areal mean temperature over the region of interest. The time series of areal mean temperatures is defined by

$$\bar{Z}_t = \frac{1}{|\mathbf{R}|} \int_{\mathbf{R}} Z_t(\mathbf{x}) \, d\mathbf{x} \quad t = 1937, \dots, 1986,$$

where $|\mathbf{R}|$ is the area of the region \mathbf{R} . Thus at each point in time, \bar{Z}_t represents the average temperature over the region during the winter starting in the December of year t and is a function of the field $Z_t(\mathbf{x})$. \bar{Z}_t provides a natural measure for the detection of changing climatic patterns over the region. As the region is devoid of gross topographic features, \bar{Z}_t provides a convenient measure of overall temperature during the winter. It is important to note that \bar{Z}_t is a characteristic of the temperature field itself and not a characteristic of the stations in the network. The behavior of the areal mean temperature will provide an indication of the overall changes in climate over the region independent of the individual stations.

Based on our model, we can summarize the available information for \bar{Z}_t from the predictive density $P(\bar{Z}_t | \mathbf{Z}_{1937}, \mathbf{Z}_{1938}, \dots, \mathbf{Z}_{1986})$; that is, the posterior density of \bar{Z}_t given the complete spatial-temporal information avail-

able. The evidence in Section 3 indicates that the temporal dependence is weak, so that $P(\bar{Z}_t | \mathbf{Z}_{1937}, \mathbf{Z}_{1938}, \dots, \mathbf{Z}_{1986})$ is very well approximated by $P(\bar{Z}_t | \mathbf{Z}_t)$. This also has the advantage of relative computational tractability.

Now

$$P(\bar{Z}_t | \mathbf{Z}_t) \propto \int_{\theta} P(\bar{Z}_t | \theta, \mathbf{Z}_t) \cdot P(\theta | \mathbf{Z}_t) \, d\theta, \quad (4.1)$$

where $P(\bar{Z}_t | \theta, \mathbf{Z}_t)$ is the predictive distribution conditional on θ and \mathbf{Z}_t , and $P(\theta | \mathbf{Z}_t)$ is the posterior distribution for the structural parameter for the year t ; see, for example, Fig. 4 for $P(\theta_2 | \mathbf{Z}_{1983})$. This calculation requires two-dimensional numerical integration for each year. Figure 8 gives the predictive distribution $P(\bar{Z}_{1983} | \mathbf{Z}_{1983})$.

By plotting the predictive distributions over time, we can observe how our knowledge of the areal mean temperature changes based on how the information in the network changes.

How can we further summarize the areal mean temperature? The distributions are symmetric and have a similar t -like distributional shape. Theoretically, the predictive distribution is a mixture of noncentral t distributions (Handcock and Stein 1993, sec. 2.3). The ratio of largest to smallest variance is 2.6. To explore further the temporal changes in \bar{Z}_t , we will consider the time series of MAP values from (4.1). Although this clearly represents a reduction in information relative to the full distribution, it does facilitate examination.

4.1 Temporal Structure of the Mean Areal Temperature

Figure 9 represents the MAP values for the last half century. Note the lack of a clear trend over time. Some interesting winters have been indicated. The last winter for which

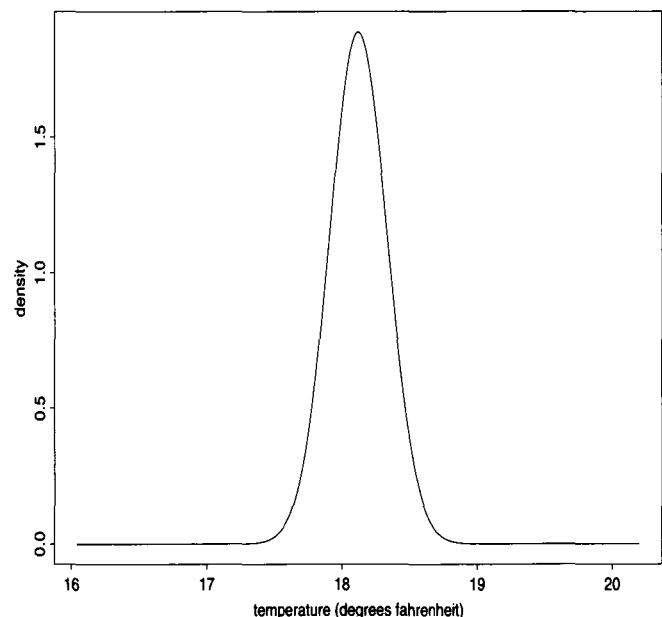


Figure 8. Predictive Distribution for the Areal Mean Temperature for Winter 1983-1984.

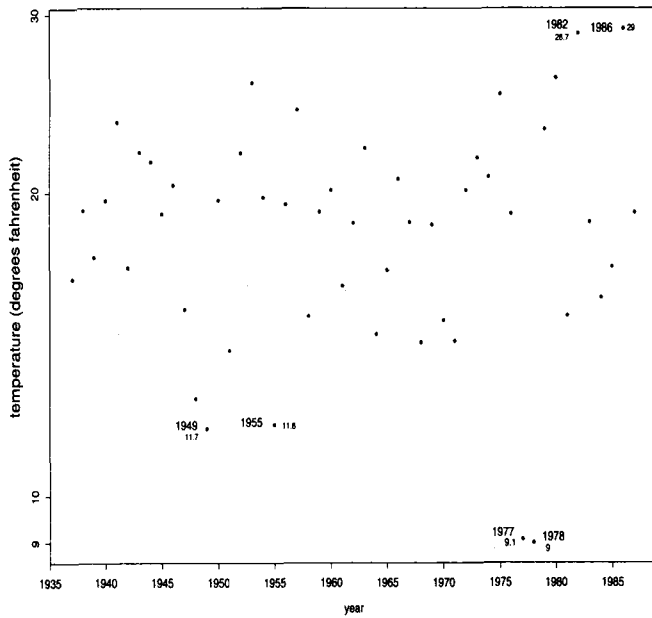


Figure 9. The Time Series of MAP Estimates for the Areal Mean Temperature. There is little short- or long-term persistence.

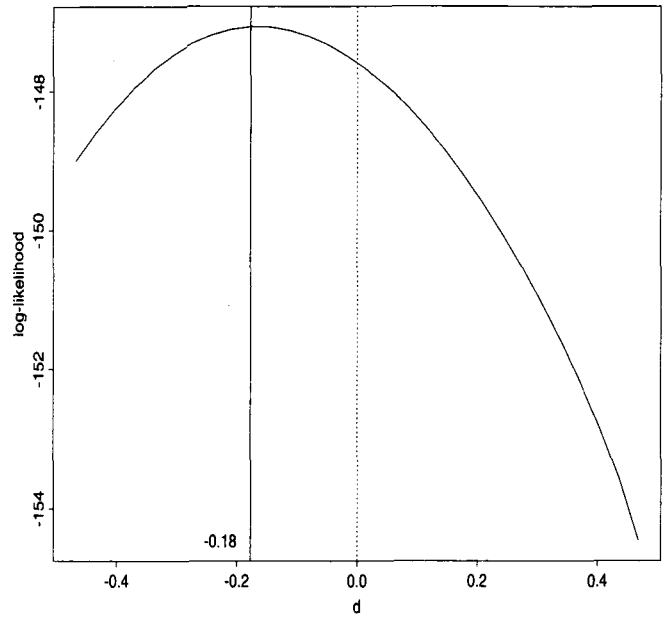


Figure 10. Profile Log-Likelihood for the Fractional Differencing Parameter, d , in the $ARIMA(0, d, 0)$ Model for the MAP Values for the Areal Mean Temperature.

data are available (1986–1987) also has the highest temperature.

Is there evidence of short- or long-term dependence in the MAP values? Using the methodology described in Section 3.1, the maximum likelihood estimator of the autocorrelation for the AR(1) model is $\hat{\rho} = .06$, with a standard error of .14. The AR(1) model provides a nonsignificant improvement in the likelihood relative to the model of independence ($\rho = 0$). The long-memory model, $ARIMA(0, d, 0)$, has an estimated fractional difference $\hat{d} = -.18$, with a standard error of .16. This provides a nonsignificant improvement in the likelihood relative to the model of independence (see Fig. 10).

Therefore, it seems that, over this period, the areal mean exhibits little evidence of temporal structure.

4.2 A Static Model for Mean Areal Temperature

A reasonable model for the mean areal temperature over the last half century is

$$\bar{Z}_t = \mu_t + \varepsilon_t \quad t = 1937, \dots, 1986, \quad (4.2)$$

where $\{\varepsilon_t\}_{t=1937}^{1986}$ is an independent identically distributed Gaussian sequence with mean 0 and variance σ^2 . The sequence $\{\mu_t\}_{t=1937}^{1986}$ represents the mean level. The motivation is the absence of strong temporal dependence (Sec. 4.1) and the approximately constant variances. The baseline model is that the means are temporally stable: $\mu_t \equiv \mu$. Here μ will be called the static areal mean temperature.

Under the model (4.2), the posterior distribution for μ from 1937 to 1986 is

$$P(\mu | \mathbf{Z}_{t_1}, \dots, \mathbf{Z}_{t_T}) \propto \int_{\bar{Z}_{t_1}, \dots, \bar{Z}_{t_T}} P(\mu | \bar{Z}_{t_k}) \times P(\bar{Z}_{t_k} | \mathbf{Z}_{t_k}) d\bar{Z}_{t_1} \dots d\bar{Z}_{t_T}.$$

The first part of the integrand can be directly calculated, and the second part is available from (4.1). As in the previous case, this requires numerical integration. Figure 11 represents the predictive distributions for the static areal mean temperature for two separate time periods. The solid line refers to 1937–1961, and the dashed line refers to 1962–1986. The mean for the first period is 20.0°F, with a standard deviation of .59°F; the mean for the second period is 19.4°F, with a

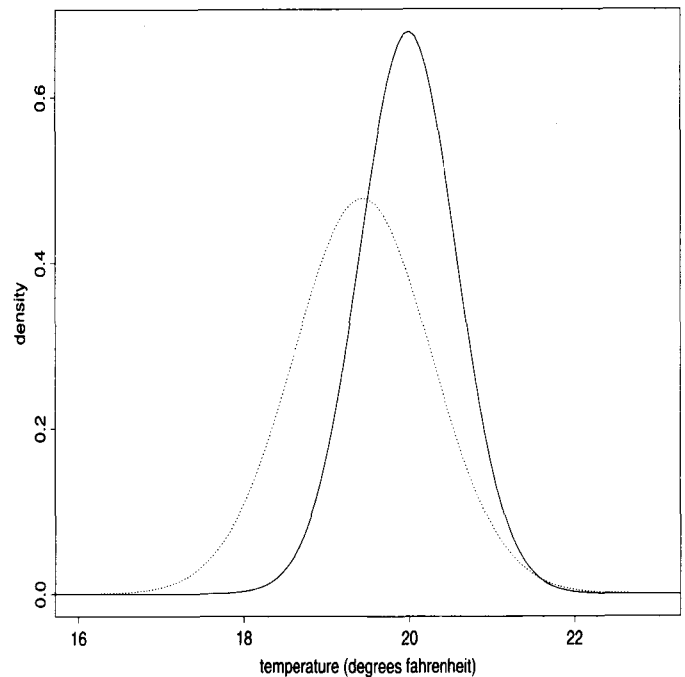


Figure 11. Predictive Distributions for the Static Areal Mean Temperature for Two Separate Time Periods. The solid line refers to 1937–1961; the dashed line, to 1962–1986.

standard deviation of $.84^{\circ}\text{F}$. These distributions summarize our uncertainty about the static areal mean temperature over each period.

Note that the distributions have substantial overlap, with the information from the later winters indicating cooler temperatures.

5. CALIBRATING CHANGES IN MEAN AREAL TEMPERATURE

The primary motivation for developing these models is to provide a tool for calibrating changes in the mean areal temperature. The model in the previous section allows this to be done. Many scenarios have been proposed for future global warming; typically, their basis is mathematical rather than empirical.

Consider the distributions in Figure 12. The solid line is the posterior distribution for the static areal mean temperature from 1937–1986. This should be compared to Figure 8; it summarizes our uncertainty about the static areal mean temperature by a distribution with mean about 19.7°F and a standard deviation of $.51^{\circ}\text{F}$.

How soon could a linear increase in static areal mean temperature in this region, totally 5°F over half a century, be discernible from the year-to-year variation?

We have a stochastic model for the phenomena that enables us to represent our uncertainty about characteristics of the phenomena. If we assume that the structure of the phenomena remains the same, except for the gradual mean shift, then we can represent the uncertainty for the unobserved data by the same structure.

Suppose that we collected data from the network in this region for the next 10 winters, as the underlying static temperature gradually increases. Suppose that besides the creep in level, the stochastic structure remained stable, as is supported by the analysis in Section 4. The dashed posterior (marked by "10") represents a hypothetical posterior for the static areal mean temperature based on that 10 winters of data. Note that there is still marked overlap with the summary from the last 50 winters (solid line). This indicates that it would be extremely difficult to discern such a gradual increase after only 10 winters.

Also plotted are the hypothetical posteriors after collecting 20, 30, and 50 winters of information. Only after about 30–40 winters is the gradual level increase discernible with high probability. If additional winters of data were available and incorporated, then the posterior would become narrower. Thus the changes would be discernible earlier than the 30–40 years indicated.

Figure 12 graphically represents the projection of the uncertainty into the future. The objective of this representation is not to decide whether warming will occur, nor to test whether it has occurred if we have 50 additional winters of data. Rather, the objective is to decide whether 50 additional winters of data will, assuming a warming scenario, allow a decision to be made within the historical variation in temperature. Under a hypothesis testing analogy, we are undertaking a power calculation, rather than conducting the statistical test itself.

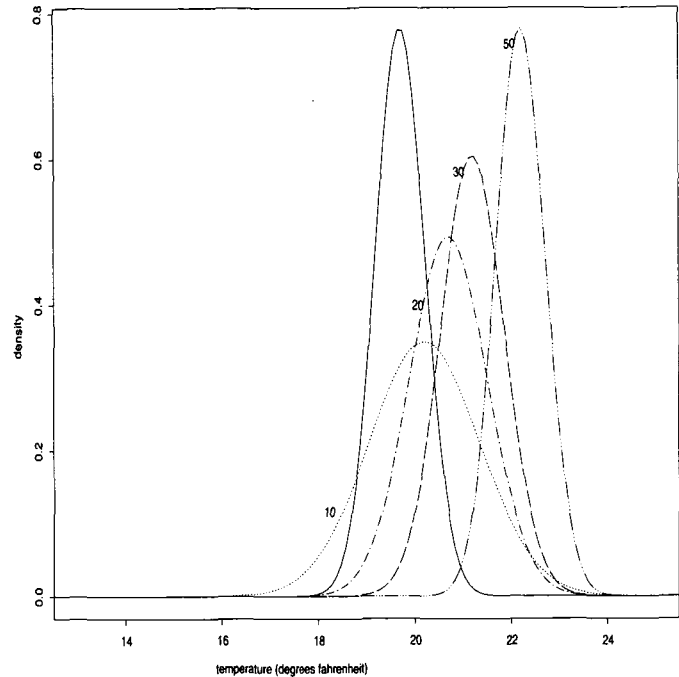


Figure 12. The Predictive Distribution for the Static Areal Mean Temperature for 1937–1986. The solid line represents a distribution based on the historical record for 1937–1986. The dashed distributions represent hypothetical posterior knowledge for the static areal mean temperature based on additional winters of data: \cdots , hypothetical for information collected over the next 10 years; $-\cdots-$, hypothetical for information collected over the next 20 years; $---$, hypothetical for information collected over the next 30 years; and $- \cdot \cdot \cdot$, hypothetical for information collected over the next 50 years.

6. CONCLUSION

Our approach facilitates the calibration of changes in the areal mean temperature against the historical record. For the scenario of a gradual increase of 5°F over 50 winters, it will take 30–40 winters of data before the change will be discernible from the natural variation in temperatures. By the time the necessary information had accumulated, an increase of $3\text{--}4^{\circ}\text{F}$ would already have occurred. The application of the model to alternative scenarios is straightforward. There is no indication that the areal mean temperature for this time of the year in this region has changed over the last half century. The observed lack of temporal trend for this region and period was somewhat of a surprise; however, this finding is consistent with that obtained using different statistical approaches (Lettenmaier, Wood and Wallis 1993). It is also evident from this later study that the results would have been quite different had other regions or periods been picked.

Similar models investigating summer temperatures and precipitation for this region will be reported elsewhere. These facilitate the measurement of runoff and hence address the central issue of the evaluation of water resources.

[Received April 1991. Revised December 1992.]

REFERENCES

- Abramowitz, M., and Stegun, I. A. (1965), *Handbook of Mathematical Functions*, New York: Dover.

- Cody, W. J. (1987), "SPECFUN—A Portable Special Function Package," in *New Computing Environments: Microcomputers in Large-Scale Scientific Computing*, ed. A. Wouk, Philadelphia: SIAM, pp. 1–12.
- Cramér, H., and Leadbetter, M. R. (1967), *Stationary and Related Stochastic Processes*, New York: John Wiley.
- Cressie, N. A. C. (1991), *Statistics for Spatial Data*, New York: John Wiley.
- Creutin, J. D., and Obled, C. (1982), "Objective Analyses and Mapping Techniques for Rainfall Fields: An Objective Comparison," *Water Resources Research*, 18, 413–431.
- Diaz, H. F., and Quayle, R. G. (1978), "The 1976–77 Winter in the Contiguous United States in Comparison With Past Records," *Monthly Weather Review*, 106, 1393–1421.
- (1980), "The Climate of the United States Since 1895: Spatial and Temporal Changes," *Monthly Weather Review*, 108, 249–266.
- Dongarra, J. J., and Du Croz, J. (1985), "Distribution of Mathematical Software Via Electronic Mail," Technical Report MCS-TM-48, Argonne National Laboratory, Mathematics and Computer Science Division.
- Gandin, L. S. (1963; 1965), *Objective Analysis of Meteorological Fields*, Leningrad: GIMIZ. Translated from Russian by R. Hardin. Israel program for Scientific Translations, Jerusalem.
- Handcock, M. S. (1989), "Inference for Spatial Gaussian Random Fields When the Objective is Prediction," unpublished Ph.D. thesis, University of Chicago, Dept. of Statistics.
- Handcock, M. S., and Stein, M. L. (1993), "A Bayesian Analysis of Kriging," *Technometrics*, 35, 4, 403–410.
- Handcock, M. S., and Wallis, J. R. (1990), "An Approach to Statistical Spatial–Temporal Modeling of Meteorological Fields," paper presented at the European Geophysical Society XV General Assembly, Copenhagen, Denmark, April 23–27, 1990.
- Haslett, J., and Raftery, A. E. (1989), "Space–Time Modeling With Long-Memory Dependence: Assessing Ireland's Wind Power Resource" (with discussion), *Journal of the Royal Statistical Society*, Ser. C, 38, 1–50.
- Hastie, T. J., and Tibshirani, R. J. (1990), *Generalized Additive Models*, London: Chapman and Hall.
- Hoeksema, R. J., and Kitanidis, P. K. (1985), "Analysis of the Spatial Structure of Properties of Selected Aquifers," *Water Resources Research*, 21, 563–572.
- Hosking, J. R. M. (1981), "Fractional Differencing," *Biometrika*, 68, 165–176.
- (1984), "Modeling Persistence In Hydrological Time Series Using Fractional Differencing," *Water Resources Research*, 12, 1898–1908.
- Intergovernmental Panel on Climate Change (IPCC) (1990), *Climate Change: The IPCC Scientific Assessment*, New York: Cambridge University Press.
- Jones, R. H. (1989), "Fitting a Stochastic Partial Differential Equation to Aquifer Head Data," *Stochastic Hydrology and Hydraulics*, 3, 100–105.
- Jones, P. D., Raper, S. C. B., Bradley, R. S., Diaz, H. F., Kelly, P. M., and Wigley, T. M. L. (1986), "Northern Hemisphere Surface Air Temperature Variations, 1851–1984," *Journal of Climate and Applied Meteorology*, 25, 161–179.
- Karl, T. R. (1985), "Perspective on Climate Change in North America During the Twentieth Century," *Physical Geography*, 6, 207–229.
- Karl, T. R., Heim, R. R., and Quayle, R. G. (1991), "The Greenhouse Effect in Central North America: If Not Now, When?," *Science*, 251, 1058–1061.
- Karl, T. R., Livezey, R. E., and Epstein, E. S. (1984), "Recent Unusual Mean Winter Temperatures Across the Contiguous United States," *Bulletin of the American Meteorology Society*, 65, 1302–1309.
- Karl, T. R., Williams, C. N., Jr., Quinlan, F. T., and Boden, T. A. (1990), "United States Historical Climatology Network (HCN) Serial Temperature and Precipitation Data," NDP-019/R1. Oak Ridge National Laboratory, Carbon Dioxide Information Analysis Center.
- Karl, T. R., Williams, C. M., Young, P. J., and Wendland, W. M. (1986), "A Model to Estimate the Time of Observation Bias Associated With Monthly Mean Maximum, Minimum and Mean Temperatures in the United States," *Journal of Climate and Applied Meteorology*, 25, 145–160.
- Kitanidis, P. K. (1983), "Statistical Estimation of Polynomial Generalized Covariance Functions and Hydrologic Applications," *Water Resources Research*, 19, 909–921.
- Kitanidis, P. K., and Lane, R. W. (1985), "Maximum Likelihood Parameter Estimation of Hydrologic Spatial Processes by the Gauss–Newton Method," *Journal of Hydrology*, 17, 31–56.
- Lettenmaier, D. P., Wood, E. F., and Wallis, J. R. (1993), "Hydrological Trends in the Continental United States," submitted to *Journal of Climate*.
- Mardia, K. V. (1989), Discussion of "Space–Time Modeling With Long-Memory Dependence: Assessing Ireland's Wind Power Resource," by J. Haslett and A. E. Raftery, *Journal of the Royal Statistical Society*, Ser. C, 38, 36–37.
- Mardia, K. V., and Marshall, R. J. (1984), "Maximum Likelihood Estimation of Models for Residual Covariance in Spatial Regression," *Biometrika*, 71, 135–146.
- Matérn, B. (1986), *Spatial Variation* (2nd ed.), Lecture Notes in Statistics, 36, Berlin: Springer-Verlag.
- Matheron, G. (1965), *Les Variables Régionalisées et leur Estimation*, Paris: Masson.
- Mejía, J. M., and Rodríguez-Iturbe, I. (1974), "On the Synthesis of Random Field Sampling From the Spectrum: An Application to the Generation of Hydrologic Spatial Processes," *Water Resources Research*, 10, 705–711.
- Mitchell, J. F. B. (1989), "The 'Greenhouse Effect' and Climate Change," *Reviews of Geophysics*, 27, 115–139.
- Omre, G. M., and Halvorsen, D. F. (1989), "A Bayesian Approach to Kriging," in *Proceedings of the Third International Geostatistics Congress I*, ed. M. Armstrong, Dordrecht: Academic Publishers, pp. 49–68.
- Quinlan, F. T., Karl, T. R., and Williams, C. N., Jr. (1987), "United States Historical Climatology Network (HCN) Serial Temperature and Precipitation Data," NDP-019, Carbon Dioxide Information Analysis Center, Oak Ridge Laboratory.
- Ripley, B. D. (1981), *Spatial Statistics*, New York: John Wiley.
- Wallis, J. R., Lettenmaier, D. P., and Wood, E. F. (1991), "A Daily Hydroclimatological Data Set for the Continental United States," *Water Resources Research*, 27, 1657–1663.
- Whittle, P. (1954), "On Stationary Processes in the Plane," *Biometrika*, 41, 434–449.
- Zimmerman, M. S., and Cressie, N. (1992), "Mean Squared Prediction Error in the Spatial Linear Model With Estimated Covariance Parameters," *Annals of the Institute of Statistical Mathematics*, 44, 27–43.
- Zimmerman, M. S., and Zimmerman, M. L. (1991), "A Comparison of Spatial Semivariogram Estimators and Corresponding Ordinary Kriging Predictors," *Technometrics*, 33, 77–91.